

# Strong collective currents of gold nanoparticles in an optical vortex lattice

R. Delgado-Buscalioni,<sup>1,2,\*</sup> M. Meléndez,<sup>1</sup> J. Luis-Hita,<sup>2,3</sup> M. I. Marqués,<sup>2</sup> and J. J. Sáenz<sup>3,4</sup>

<sup>1</sup>*Department of Theoretical Condensed Matter Physics,  
Universidad Autónoma de Madrid, 28049 Madrid, Spain*

<sup>2</sup>*Condensed Matter Physics Center (IFIMAC),  
Universidad Autónoma de Madrid, 28049 Madrid, Spain*

<sup>3</sup>*Donostia International Physics Center (DIPC),  
Paseo Manuel Lardizabal 4, 20018 Donostia-San Sebastian, Spain*

<sup>4</sup>*IKERBASQUE, Basque Foundation for Science, 48013 Bilbao, Spain*

(Dated: today)

## Abstract

Self-organized collective behaviour of active units is inspiring new designs of artificial swarms of micron-sized objects, like colloidal micro-rollers under magnetic fields coupled via hydrodynamics, or optically active colloids superdiffusing at microns per second due to multiple scattering in random, time-dependent fields. However, active control at the nanoscale remains elusive. We have accurately solved the collective optofluidic dynamics of gold plasmonic 50 nm-radius nanoparticles moving in aqueous solution under a nonconservative optical field created by the intersection of two perpendicular coherent laser beams and the resulting multiple scattering. Above a critical field intensity and a very dilute critical concentration, an interplay between optical forces, thermal fluctuations and hydrodynamic pairing leads to a spontaneous transition towards synchronised motion exhibiting a rich assortment of collective dynamics. The critical phenomenon creates strong unidirectional currents of nanoparticles, reaching speeds of centimeters per second along the diagonals of the lattice. This stationary optical field is experimentally feasible and can provide new ways to control mixing and mass and heat transport at the nanoscale.

From bacteria to birds, patterns of synchronised collective motion are ubiquitous in nature[1–3]. Remarkably, these patterns are reproduced by simple models which need only an interaction mechanism and some form of activation [4]. Such simplicity reveals the universal character of collective behaviour and inspires new designs of micron-size artificial swarms [1, 5, 6]. Colloidal rollers, coupled through hydrodynamics and activated by electric [6] or magnetic [5] fields move in flocks, with clusters speeds of centimeters per second [5]. Optically active micron-sized particles super-diffuse at microns per second under random multiple scattering [7, 8]. However, due to thermal fluctuations, active control becomes elusive at the nanoscale [1]. We present detailed numerical solutions of a new class of optically controlled active media on *time stationary fields* of curl-forces [9–11] acting on 50 nm gold nanoparticles. We find a new critical phenomenon arising from the interplay between optic forces, thermal fluctuations and hydrodynamic pairing [12] which creates high-speed (centimetres per second) jets and other nanoparticle currents. Our setup suggests new ways for nanoscale heat transport and mixing and stimulates theoretical questions on pattern selection in thermal systems out of equilibrium.

We consider a suspension of  $N$  gold nanoparticles (NP) of  $R = 50$  nm radius in water at an extremely dilute volume fraction ( $\phi = 4\pi R^3 N / (3V) \sim 10^{-4}$ ) exposed to a nonconservative optical field formed by the intersection of two perpendicular coherent laser beams pointing in the  $x$  and  $y$  directions (optic plane), respectively, and polarized in the  $z$  direction with a phase difference  $\theta = \pi/2$  rad (see Fig. ??). This *primary* field with wavelength  $\lambda$  and wavenumber  $k = 2\pi/\lambda$  [13] equals  $\mathbf{E}_0(\mathbf{r}) = i2|E_0|(\sin(kx) + e^{i\theta}\sin(ky))\hat{\mathbf{z}}$  with  $|E_0|^2 = 2In/(c\epsilon\epsilon_0)$  controlled by the power density intensity of the laser beam  $I$  and the refractive index of water  $n = \sqrt{\epsilon}$  ( $\epsilon$  stands for the macroscopic permittivity and  $c$  for the speed of light). For spherical nanoparticles much smaller than the laser wavelength  $R \ll \lambda$  it is safe to use the electric dipole approximation providing a complex electrical polarizability  $\alpha = \alpha' + i\alpha''$  given by the Clausius-Mossotti relation [14] and the radiative correction term (see Supplementary Information, SI) which depends on the relative permittivities of water  $\epsilon$  and gold  $\epsilon_p(\omega)$ . The particles are not charged but the spatially modulated field  $\mathbf{E}_{exc}$  will induce a dipole  $\mathbf{p}_i = \epsilon\epsilon_0\alpha\mathbf{E}_{exc}(\mathbf{r}_i)$  centered on the position of each particle  $\mathbf{r}_i$  and, consequently a non-vanishing averaged Lorentz force with components  $\mathbf{F}(\mathbf{r}_i) = (\epsilon\epsilon_0/2) \text{Re} \{ \alpha [\mathbf{E}_{exc}(\mathbf{r}) \cdot \nabla \mathbf{E}_{exc}^*(\mathbf{r})] \}_{\mathbf{r}=\mathbf{r}_i}$ . The

primary optical force stems from the primary field  $\mathbf{E}_{\text{exc}} = \mathbf{E}_0$ ,

$$\begin{aligned} \mathbf{F}^{(1)}(x, y) = & 2\alpha' \frac{n}{c} I \nabla (\sin^2(kx) + \sin^2(ky)) \\ & + 2\alpha'' \frac{n}{c} I \nabla \times [2 \cos(kx) \cos(ky) \mathbf{e}_z]. \end{aligned} \quad (1)$$

This force field (1) forms a periodic pattern of optical vortices [15], with a Bravais unit cell in  $(x, y) \in [-\lambda/2, \lambda/2]$  (see Fig. 1(b)). Its non-conservative part  $\nabla \times A(x, y)\hat{\mathbf{z}}$ , proportional to  $\alpha''$  [16], embodies the so-called ‘‘curl forces’’ [9–11]. It resembles a checkerboard, with alternating squares of positive and negative vorticity. Curl-forces neatly convert the laser energy into work [9, 10, 17] and  $U \equiv 2I(n/c)\alpha'' = \epsilon\epsilon_0|E_0|^2\alpha''$  (related to the energy per NP) is a convenient unit to compare with the thermal counterpart  $k_B T$ .

The primary field has no stationary nodes where the NP can rest [18], but four unstable saddle nodes (SD) instead (see Fig. 1(b)). As a consequence, an isolated gold NP undergoes giant normal diffusion when exposed to this primary optical field [19, 20]. The NP moves quickly along the edges of the vortices, following one of the four fast tracks connecting unstable SDs, and then slows down close to the SD, where  $\mathbf{F}^{(1)} = 0$ . Thermal agitation forces the NP to leave the saddle node by *randomly* picking one of the unstable directions towards another SD, where the process repeats. These dynamics creates curved paths of NPs around the vortex cores and enhance their diffusion. A nanoparticle moves without inertia (Stokesian regime) with a self-mobility  $\mu_0 = (6\pi\eta R)^{-1}$  where  $\eta$  represents the fluid viscosity. The fluid drag balances the primary force (1),  $F^{(1)} \sim U/\lambda$ , providing a *self*-contribution to its velocity  $v_i^{(s)} = \mu_0 F_i^{(1)}$ . The NP crosses a  $\lambda/2$  lattice edge in a time  $\tau_{op} \sim \lambda/v_i^{(s)}$  thus providing a diffusion coefficient  $D_{op} \sim \lambda^2/\tau_{op} = u D_{th}$  which is larger than the thermal value  $D_{th} = k_B T \mu_0$  for  $u \equiv U/k_B T > 1$ . This nondimensional laser energy  $u$  can be increased up to  $\sim 10^2$  before cavitation takes place [21, 22].

We investigate the *collective behaviour* of a *suspension* of gold NPs. Aside from the primary force in Eq. (1) and the thermal kicks, NPs interact optically through multiple scattering forces  $\mathbf{F}^{(2)}(\{\mathbf{r}\})$ , and also hydrodynamically, with a collective drag velocity  $\mathbf{v}_i^{(c)} = \sum_j \mu_{ij}(r_{ij})\mathbf{F}_j$  arising from the *mutual* hydrodynamic mobility  $\mu_{ij}$  dominated by the Oseen term  $\mu_{ij} \sim 1/r_{ij}$ . While hydrodynamics propagates forces to velocities, the optical Green function  $G$  propagates light to forces (see SI) and is also long-ranged  $G \sim 1/r_{12}$ .

In order to isolate the effect of hydrodynamic interactions (HI) at fixed  $\phi$ , we first solved

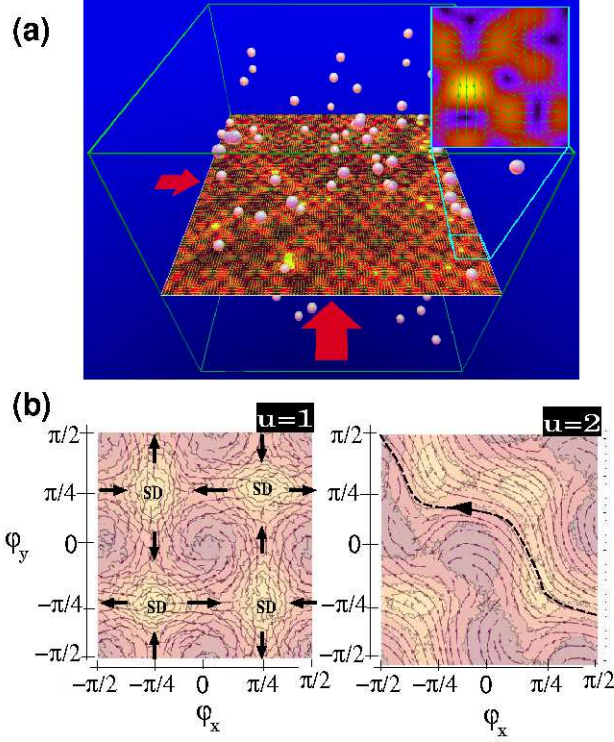


FIG. 1: (a) Suspension of gold nanoparticles in the intersection of two coherent laser beams (red arrows) with  $\lambda = 395$  nm polarized in the  $z$  (vertical) direction and propagating in  $x$  and  $y$  directions (optic plane) with a  $\pi/2$  rad phase lag. The nanoparticle (NP) radius is  $R = 50$  nm. The figure illustrates a fixed- $z$  cross section of the force field and the modulus of the total electric field  $|E|$  including the incident beams and the contribution to the light scattered by each NP (brighter regions mean higher  $|E|$ ). In this setup, the NPs remain confined to a cubic box of side  $L \simeq 7.0\lambda$ . (b) Isocontours of single-particle probability density and streamlines of the NP velocity field in a periodic domain, folded into the Bravais unit cell of the primary optic field  $x \in [-\lambda/2, \lambda/2]$  (same for  $y$ ) against phase-coordinates  $\varphi_x = 2\pi(x/\lambda)$ . The non-dimensional laser energy (see text) corresponds to  $u = 1$  (below)  $u = 2$  (above) the transition to coherent NP motion (volume fraction  $\phi = 3.0 \times 10^{-3}$ ). Brighter regions correspond to denser domains. The unstable saddle nodes (SD) of the primary force field (Eq. 1) are indicated in the  $u = 1$  panel. The dashed line for  $u = 2$  illustrates a zig-zag path followed by NPs under coherent dynamics.

these dynamics under periodic boundary conditions (PBC), without taking into account multiple scattering. These dynamics were solved using the Fluctuating Immersed Boundary method (FIB), which is an immersed boundary method for Stokesian particles in fluctuating hydrodynamics [23] (see SI). We evaluate the (time dependent) single particle diffusion defined as,  $D(t) = \Delta_1^2/(4t)$  where  $\Delta_1^2 = \langle (\mathbf{r}_1^{\parallel}(t_0 + t) - \mathbf{r}_1^{\parallel}(t_0))^2 \rangle$  is the in-plane ( $\parallel$ ) mean square displacement (MSD) of a tracer NP with position  $\mathbf{r}_1 = \mathbf{r}_1^{\parallel} + z_1 \hat{\mathbf{e}}_z$ . At a fixed  $\phi$ , Fig. 2(a) shows a sudden transition from (enhanced) normal diffusion  $D = D_{op}$  to superdiffusion  $D(t) \sim t^\beta$ , where the diffusion exponent jumps to the ballistic value  $\beta = 1$  above the critical laser energy  $u > u_{cr}(\phi)$ .

The phase diagram of Fig. 2(d) draws the critical line  $(u_{cr}, \phi_{cr})$  separating uncorrelated walkers from a synchronized flow of NPs. This line satisfies by the relation  $\xi^* = (u_{cr} - u^*)(\phi_{cr} - \phi^*)$  where  $u^*$  and  $\phi^*$  are threshold values below which the transition does not occur. Under PBC we find  $\xi^* = (1.55 \pm 0.05) \times 10^{-4}$  while  $\phi^* = (1.5 \pm 0.1)^{-4}$  and  $u^* = 1.0$ . Interestingly, coherent dynamics cannot ensue unless the energy per NP  $U$  surpasses the thermal energy  $U > U^* \simeq k_B T$ . Also remarkable, is the low threshold concentration  $\phi^*$  involving an average separation of  $3\lambda$  between NPs. The coherent dynamics in periodic boundaries leads to the formation of a large vortex of NPs occupying the whole box in  $z$  direction and flowing with vorticity in  $\mathbf{d}$  direction. A somewhat similar rotating flow would take place in an enclosure with walls. This *3D roll* is illustrated in Fig. 2(c). As indicated in the phase diagram of 2(d), at larger  $u$  or  $\phi$  an extremely rich collective dynamics unfolds (more details in SI).

To investigate the effect of multiple scattering we calculate the many-body secondary optic forces  $\mathbf{F}_2(\mathbf{r})$  (see SI) and plugged them into a Brownian solver implemented with the Rotne-Prager-Yamakawa mobility tensor for HI [24]. To fix  $\phi$  we first considered a confined domain where a repulsive external potential impedes NPs from escaping out from a cubic box of side  $L = 7\lambda$ . This confined geometry mimics an experimentally feasible laser-trap [25]. In this case we analyzed the collective diffusion evaluated from the in-plane displacement of the center of mass (CoM) of the NP ensemble  $D_{cm}(t) = \Delta_{cm}^2(t)/(4t)$  (details in the SI). Under confinement, the onset of the superdiffusive regime  $D_{cm} \sim t^\beta$  matches what found under PBC, highlighting the hydrodynamic nature of the transition. Figure 2(b) plots values of  $\beta$  (for both periodic and confined domains) against the governing non-dimensional group  $\xi \equiv [u_{cr}(\phi) - u][\phi_{cr}(u) - \phi]$ . The transition is sharp and resembles the first-order dynamic

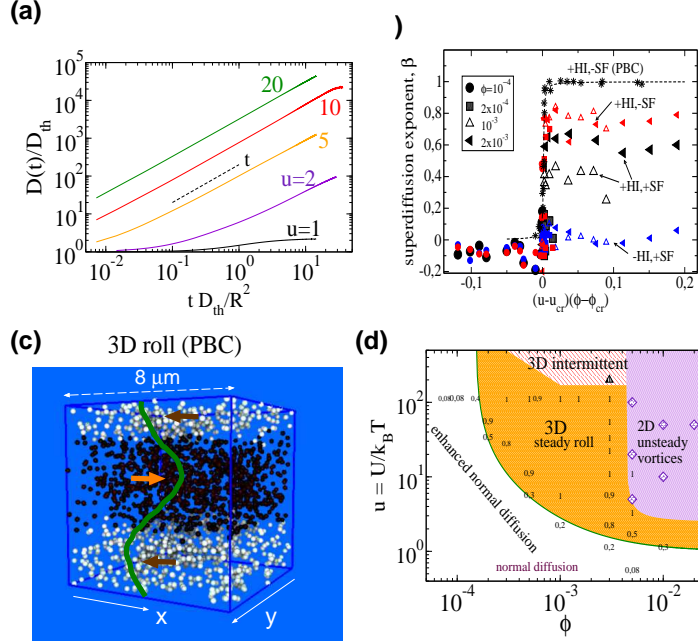


FIG. 2: (a) Effective diffusion of gold NPs  $D(t) = \Delta_1^2/(4t)$  obtained from their in-plane mean square displacement  $\Delta_1^2$  and scaled with the thermal value  $D_{th} = k_B T/\mu_0$  with  $\mu_0 = 1/(6\pi\eta R)$ . For  $U/K_B T = u > u_{cr} \sim 1$  the NP dynamics become ballistic  $D \sim t^\beta$  with  $\beta = 1$ . (a) corresponds to periodic boundaries (PBC) where scattering forces are not taken into account. (b) Diffusion of the center of mass of NPs confined in a cubic domain of size  $7.0\lambda$ , calculated from in-plane displacements  $D_{cm} = \Delta_{cm}^2/(4t)$ . The diffusive exponent  $\beta$  is measured at intermediate times  $\tau_{op} < t < \tau_\Delta$  (indicated with the dashed lines below the values of  $\beta$ ). (c) The exponent  $\beta$  against the governing parameter  $\xi = [u - u_{cr}(\phi)][\phi - \phi_{cr}(u)]$  for PBC and confined setups, comparing results with and without hydrodynamic interactions (+HI and -HI) and/or secondary optical forces (+SF and -SF). (d) The dynamic phase diagram showing the transition from enhanced diffusion ( $D \simeq uD_{th}$ ) to coherent dynamics  $D \sim t^\beta$ . (green) is given by  $\xi^* = (u_{cr} - u^*)(\phi_{cr} - \phi^*)$  (see text for details).

transition reported for the Vicsek model [26]. Confinement increases the value of the critical parameter to  $\xi^* = (6 \pm 1) \times 10^{-4}$ , but it does not alter the shape of the critical line nor significantly modifies the thresholds values ( $u^* \simeq 0.7$  and  $\phi \simeq (1.1 \pm 0.01) \times 10^{-4}$ ), suggesting a sort of “material property”, as it was mentioned for micro-rollers collective dynamics [6].

The “microscopic” origin of the coherent dynamics can be understood by plotting the single-NP probability density  $\rho(\mathbf{r})$  and the streamlines of the NP average current, in Fig.

1(b). Above the critical energy, i.e.  $u = 2$  in Fig.1(b), superdiffusion arises as an instability of the basic stationary solution  $\rho_0(\mathbf{r})$ , which corresponds to  $u = 1$  in Fig.1(b). The instability is triggered by the collective current  $\mathbf{v}^{(c)}$  arising from hydrodynamic couplings between NPs. As shown in 1(b), this current breaks one symmetries of the primary optical field (mirrored by  $\rho_0(\mathbf{r})$ ) and creates an average mass flow across the system. The particles tend to follow each other along zig-zag paths which move along one of the four possible diagonal directions of the lattice  $\mathbf{d} = (\pm 1, \pm 1)$ . This is consistent with hydrodynamic pairing [12] which is known to happen if particles are forced to follow curved paths in a liquid. Note that the instability is degenerate in  $\mathbf{d}$  and the NP current might jump from one diagonal to another, after many optical times  $\tau_{op}$ .

Although the dynamic transition stem chiefly from hydrodynamic interactions (HI), secondary forces have a measurable effect in reducing the intensity of the collective current. Secondary forces may be viewed as a self-generated, speckle intensity pattern induced by multiple scattering of light, added to and severely disrupting the periodic stationary pattern of the curl force field and, in turn, reducing the coherence of the zig-zag paths under coherent motion (see Fig 3(b)). The phase lag term  $\exp[i\mathbf{k} \cdot \mathbf{r}_{ij}]$  present in the optical Green function (see SI) creates undulating force patterns [27] which become quite complex, even for just two isolated NPs  $\mathbf{F}^{(2)} = \mathbf{F}^{(2)}(\mathbf{r}_1, \mathbf{r}_2)$  (see Fig.3(a) and Video 3). As illustrated in Fig. 3(a), two NPs in the same optic plane tend to repel each other. In a confined domain (see SI), this leads to the expansion of the NP's ensemble volume. However, along  $z$ , the scatter produces marginally stable domains [ $F_z = 0$  and  $dF_z/dz < 0$ , see Fig. ??(b)] which, in suspension, creates transient layers of NPs separated by roughly  $\Delta z \sim 2\lambda$  [SI and Fig. 4(b)].

A nontrivial question is what happens if the confinement is removed. As a possible outcome, the extra pressure from secondary forces might destruct coherent motion by inducing a fast dispersion of NPs over the optic plane. We prepared experiments placing NPs in the confined domain, with  $u$  and initial concentration  $\phi(t = 0)$  above the transition line. By contrast, upon removing the confining potential we immediately observe the formation of a jet of NPs moving at a surprisingly large velocity. The trajectories of single NPs, the CoM displacement and velocity  $v_{cm}(t)$  are shown in Fig. 4 for one of the cases considered. The jet moves along one the diagonals  $\mathbf{d}$  and its direction remains stable until dispersion (mostly along  $\mathbf{d}$  direction) decreases the concentration of NPs below the critical value  $\phi(t) < \phi_{cr}(u)$  [see Fig. 4(b)]. Notably, the flock disperses much less in  $z$  direction when secondary forces

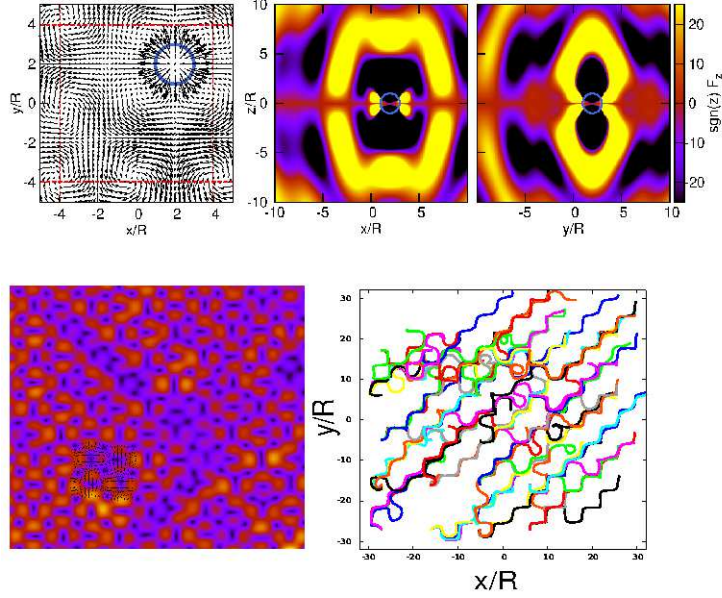


FIG. 3: (a) The force field on particle  $i = 2$ , in a two-NPs configuration,  $\mathbf{F}_2 = \mathbf{F}_2^{(1)}(\mathbf{r}_2) + \mathbf{F}_2^{(2)}(\mathbf{r}_1, \mathbf{r}_2)$ , where  $\mathbf{F}_2^{(2)}$  comes from the light scattered by NP  $i = 1$ , located at  $z = 0$  and plane location  $(1/4, 1/4)\lambda$  (blue circle). The dotted red lines indicate a separation of  $\lambda$ . *Centre, right* plots, for the same case, the normal component of the optical force  $F_z$  in the  $xz$  and  $yz$  planes times the sign of  $z$  (i.e. if  $\text{sgn}(z)F_z < 0$  the force is attractive and viceversa). Red contours, around  $z \simeq \pm\lambda = \pm 7.9 R$  correspond to “stable” domains where  $F_z = 0$  and  $dF_z(z)/dz < 0$ . Values of  $F_z$  saturate to black and yellow beyond the values indicated in the colour scale. Panel (b) and (c) shows a cut at  $z = 0$  of the total electric field intensity  $|E(\mathbf{r}, t_0)|$  obtained from  $\phi = 3 \times 10^{-3}$  and  $u = 2$ . Panel (c) illustrates the trajectories of the NPs close to this  $z = 0$  plane and time  $t = t_0$ . Disruptions of the zig-zag paths due to scattering interactions correlate with the dislocations of the  $\mathbf{E}$  lattice pattern.

are added. In fact, attractive secondary forces in  $z$  direction counter-balance the repulsive hydrodynamic mutual drag in  $z$  direction [28] As shown in Fig. 4(c) and (d) the collective velocity scales like  $v_{cm} \propto (\phi - \phi_{cr})^{1/3}$  which differs from that observed in collective motion of microrollers  $v_{cm} \sim (\phi - \phi_{cr})$  [5, 6]. A simple scaling argument unifies both results. In terms of the interparticle distance  $r_{12}$ , the leading term in the mutual mobility generally scales like  $\mu_{12} \sim 1/r_{12}^\alpha$  while, in a  $d$ -dimensional system,  $r_{12} \sim \phi^{-1/d}$ . One thus expects the collective velocity  $v_{cm} \sim \mu_{12}F_2$  to scale like  $v_{cm} \sim \phi^{\alpha/d} F$ . Groups of microrollers move with  $v_{cm} \sim \phi$

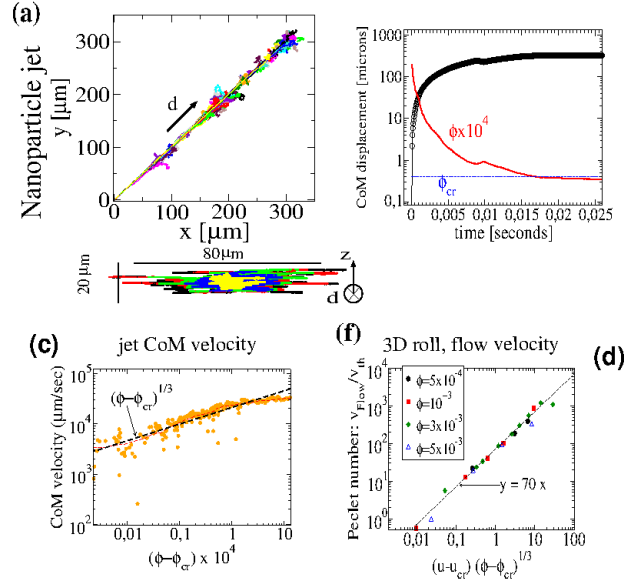


FIG. 4: Nanoparticle jet: (a) Trajectories in the optic plane of 80 nanoparticles after being released from their confinement in a box of  $L \simeq 2.9 \mu\text{m}$  (different colors for different NPs). (b) Displacement of the center of mass (CoM) and (c) the CoM velocity  $v_{cm}$  versus the instantaneous volume fraction  $\phi(t)$  (measured from the NP's ensemble volume  $\mathcal{V} = \prod_{\alpha} R_{\alpha}^{1/2}$ , where  $\mathbf{R}$  are the eigenvalues of the ensemble's gyration tensor). The scaling  $v_{cm} \sim (\phi - \phi_{cr})^{1/3}$ . is consistent with the master curve (d) showing the peak of the velocity profile of the 3D roll NP-flow in a periodic domain (without secondary forces)

$$v_{\text{Flow}} \propto (u - u_{cr}) (\phi - \phi_{cr})^{1/3}$$

[5, 6] close to a wall, where  $d = 2$  and  $\alpha = 2$ . In our setup  $d = 3$  and the laser force  $F \sim U/\lambda$  activates monopole (Oseen) couplings  $\alpha = 1$ , providing  $v_{cm} \sim \phi^{1/3}U/\lambda$ . To complete our scaling, we impose  $v_{cm} = 0$  below the critical line, leading to  $v_{cm} \propto (u - u_{cr}) (\phi - \phi_{cr})^{1/3}$  which agrees quite well with results in periodic and unconfined domains, as shown in Fig. 4(c) and (d).

We have presented a collective dynamic transition of optically driven gold nanoparticles, which shares many generic features of (deterministic) micron-sized active colloidal flocks [5, 6]. By contrast, here, thermal forces are strong but also essential to trigger the collective dynamics. Without fluctuations the NPs would freeze at the saddle nodes and under extreme energies  $u > 200$  NPs take too long to leave the SD domains, leading to intermittency and suppression of collective motion (see Fig. 2(d) and SI). This is strongly reminiscent of

*stochastic resonance* [29] (SR) where fluctuations trigger coherent dynamics within a finite window of noise amplitudes. Optically active microparticles interacting in a time-varying fluctuating speckle light field diffuse about three times faster than thermally  $D_{th}$ , moving at microns per second [7, 8]. Here, stochastic forces “excite” NP displacements in a *stationary optical field* leading to strong (monopolar) hydrodynamics driving jets of *nanoparticles* at velocities of centimeters per second, similar to micro-rollers clusters [5]. The required power densities are standard for optical tweezers [27],  $I \sim 10^9$  W/m<sup>2</sup> attained by focusing a 0.1 W laser onto a  $\sim 10$   $\mu$ m-side domain. Close to the plasmon resonance, local heating is expected upon increasing  $I$  [22, 30] so these dynamics might then provide a new way for ultrafast transport of heat at the nanoscale [31]. Also, in our setup the nanoscopic-length Peclet number  $v_{cm}R\rho_f/\eta$  reaches the hundreds range, promising a novel route for rapid mixing in microdroplets [32].

## ACKNOWLEDGEMENTS

This research was supported by the Spanish Ministerio de Economía y Competitividad (MICINN) and European Regional Development Fund (ERDF) through Projects Explora NANOMIX FIS2013-50510-EXP, FIS2015-69295-C3-3-P and the Basque Dep. de Educación through Project PI-2016-1-0041 (J.J.S.). .

---

\* [rafael.delgado@uam.es](mailto:rafael.delgado@uam.es)

- [1] C. Bechinger, R. Di Leonardo, H. Löwen, C. Reichhardt, G. Volpe, and G. Volpe, *Reviews of Modern Physics* **88**, 045006 (2016).
- [2] G. Theraulaz, E. Bonabeau, S. C. Nicolis, R. V. Solórzano, V. Fourcassié, S. Blanco, R. Fournier, J.-L. Joly, P. Fernández, A. Grimal, et al., *Proceedings of the National Academy of Sciences of the United States of America* **99**, 9645–9649 (2002), ISSN 0027-8424, URL <http://europepmc.org/articles/PMC124961>.
- [3] A. D. Buscalioni, A. de la Iglesia, R. Delgado-Buscalioni, and A. Dejoan, in *Modularity*, edited by W. Callebaut and D. Raskin (MIT press, 2005).
- [4] T. Vicsek and A. Zafeiris, *Physics Reports* **517**, 71 (2012).

- [5] M. Driscoll, B. Delmotte, M. Youssef, S. Scanna, A. Deonve, and P. Chaikin, *Nature Physics* **13**, 375 (2017).
- [6] A. Bricard, J.-B. Caussin, N. Desreumaux, O. Dauchot, and D. Bartolo, *Nature* **503**, 95 (2013).
- [7] K. M. Douglass, S. Sukhov, and A. Dogariu, *Nature Photonics* **6**, 834 (2012).
- [8] G. Volpe, G. Volpe, and S. Gigan, *Scientific Reports* **4**, 3936 (2014).
- [9] M. V. Berry and P. Shukla, *Journal of Physics A: Mathematical and Theoretical* **46**, 422001 (2013).
- [10] M. V. Berry and P. Shukla, *Proceedings of the Royal Society of London A: Mathematical, Physical and Engineering Sciences* **471** (2015).
- [11] R. Gómez-Medina, M. Nieto-Vesperinas, and J. J. Sáenz, *Physical Review A* **83**, 033825 (2011).
- [12] Y. Sokolov, D. Frydel, D. G. Grier, H. Diamant, and Y. Roichman, *Physical review letters* **107**, 158302 (2011).
- [13] S. Albaladejo, M. I. Marqués, F. Scheffold, and J. J. Sáenz, *Nanoletters* **9**, 3527 (2009).
- [14] L. Novotny and B. Hecht, *Principles of Nano-Optics* (Cambridge University Press, Cambridge, 2006).
- [15] I. Zapata, R. Delgado-Buscalioni, and J. J. Sáenz, arXiv preprint arXiv:1510.08664 (2015).
- [16] Note1, to maximize the ratio  $|\alpha''|/|\alpha'|$  we consider a wavelength close to the gold plasmon resonance in water  $\lambda \approx 395$  nm, setting  $\epsilon = 1.8$ ,  $\alpha' \approx 1 \times 10^{-21}$  m<sup>3</sup> and  $\alpha'' \approx 2\alpha'$ .
- [17] A. Hemmerich and T. Hänsch, *Physical review letters* **68**, 1492 (1992).
- [18] I. Zapata, S. Albaladejo, J. M. R. Parrondo, J. J. Sáenz, and F. Sols, *Physical Review Letters* **103**, 130601 (2009).
- [19] S. Albaladejo, M. I. Marqués, and J. Sáenz, *Opt. Express* **19**, 11471 (2011).
- [20] S. Albaladejo, M. I. Marqués, M. Laroche, and J. J. Sáenz, *Physical Review Letters* **102**, 113602 (2009).
- [21] Y. Sivan and S.-W. Chu, *Nanophotonics* **6**, 317 (2017).
- [22] Y. Seol, A. E. Carpenter, and T. T. Perkins, *Optics letters* **31**, 2429 (2006).
- [23] S. Delong, F. B. Usabiaga, R. Delgado-Buscalioni, B. E. Griffith, and A. Donev, *The Journal of chemical physics* **140**, 134110 (2014).
- [24] D. L. Ermak and J. McCammon, *J. Chem. Phys.* **69**, 1352 (1978).
- [25] M. Dienerowitz, M. Mazilu, P. J. Reece, T. F. Krauss, and K. Dholakia, *Optics Express* **16**, 4991 (2008).

- [26] G. Gregoire and H. Chate, Phys. Rev. Lett. **92**, 025702 (2012).
- [27] G. Brügger, L. S. Froufe Pérez, F. Scheffold, and J. J. Sáenz, Nature Communications **6**, 7460 (2015).
- [28] Note2, the  $z$  component of the Oseen drag on particle  $i = 1$  due to another one  $j = 2$  moving in a different optic plane ( $\mathbf{r}_{12} = \mathbf{r}_{\parallel} + z\hat{\mathbf{e}}_z$ ) is  $\hat{\mathbf{e}}_z \cdot \boldsymbol{\mu}_{12} \cdot \mathbf{F}_2 \propto -(z/r)\mathbf{F}_2 \cdot \hat{\mathbf{r}}_{\parallel}$  where  $\mu_{ij}(r_{ij}) = 1/(8\pi\eta r_{ij})(\mathbf{I} + \mathbf{r}_{ij}\mathbf{r}_{ij}/r_{ij}^2)$ . This drag pushes both particles away in  $z$  direction.
- [29] L. Gammaitoni, P. Hänggi, P. Jung, and F. Marchesoni, Reviews of Modern Physics **70**, 223 (1998).
- [30] O. A. Yeshchenko, N. V. Kutsevol, and A. P. Naumenko, Plasmonics **11**, 345 (2016).
- [31] G. Baffou and R. Quidant, Laser & Photonics Reviews **7**, 171 (2013).
- [32] W. H. Chong, L. K. Chin, R. L. S. Tan, H. Wang, A. Q. Liu, and H. Chen, Angew. Chem. Int. Ed. **52**, 8750 (2013).